Modulating Light-Tunable Acid Sensitivity of a Bioinspired Polymer Simply by Adjusting the Position of a Single Methoxy Substituent

Zhilin Liu,[1,2] Yufang Tang,[2] Nan Li,[2] Lican Lu,[2] Junjie Deng,[1] Yuanli Cai[1,2]

[1]Jiangsu Key Laboratory of Advanced Functional Polymer Design and Application, Department of Polymer Science and Engineering, College of Chemistry, Chemical Engineering and Materials Science, Soochow University, Suzhou 215123, China
[2]Key Laboratory of Environmentally Friendly Chemistry and Applications of Ministry of Education, and Key Laboratory of Advanced Functional Polymeric Materials of College of Hunan Province, College of Chemistry, Xiangtan University, Xiangtan 411105, China
Correspondence to: Y. Cai (E-mail: ylcai@suda.edu.cn)

Received 10 August 2011; accepted 9 October 2011; published online 7 November 2011
DOI: 10.1002/pola.25057

ABSTRACT: This article describes a rhodopsin-inspired photosensitive polymer whose light-tunable acid sensitivity can be widely modulated simply by adjusting the position of a single methoxy substituent in the aromatic rings of cinnamyl groups. The well-defined poly(5-ethyl-5-methacryloyloxymethyl-2-(*p*-methoxystyryl)-[1,3]dioxane) (PEM*p*MSD) and poly(5-ethyl-5-methacryloyloxymethyl-2-(*o*-methoxystyryl)-[1,3]dioxane) (PEM*o*MSD) as well as poly(5-ethyl-5-methacryloyloxymethyl-2-styryl-[1,3]dioxane) were synthesized via reversible addition-fragmentation chain transfer (RAFT) process. The results demonstrated that the *para*-methoxy substitution of EM*p*MSD monomer led to the more shortened initialization period and rapid chain propagation of RAFT process than 5-ethyl-5-methacryloyloxymethyl-2-styryl-[1,3]dioxane monomer under mild visible light radiation at 25 °C. The *ortho*-methoxy substitution of PEM*o*MSD led to high degree of photoinduced *Z*-isomerization over 80%. Moreover, the *para*-methoxy substitution of PEM*p*MSD led to the rapid hydrolysis of the cyclic acetal linkages in ambient acid media, while the *ortho*-methoxy substitution of PEM*o*MSD slowed down this hydrolysis. This hydrolysis slowed down on *Z*-isomerization particularly in PEM*o*MSD. These effects widely broadened the tunability of the light-modulated acid sensitivity. © 2011 Wiley Periodicals, Inc. J Polym Sci Part A: Polym Chem 50: 495–508, 2012

KEYWORDS: biomimetic; reversible addition fragmentation chain transfer (RAFT); stimuli-sensitive polymers; structure-property relations

INTRODUCTION Stimulus-responsive polymers are playing increasingly important roles in a variety of fields.[1,2] Among them, photosensitive polymers have various applications ranging from reversible optical data storage,[3,4] polymer viscosity control,[5] photomechanical actuation,[6] bioactivity switching of proteins,[7] tissue engineering,[8] drug delivery,[9] etc. Recently, the light-triggered aggregation and dissociation of polymers were extensively studied.[10–13] The majority of chemistry used relied on the photoisomerization of azobenzene[10,14–22] or spiropyran[23–25] moieties. Another viable chemistry was the cleavage of photolabile groups. Zhao[26–29] and other groups[30–32] described the dissociation of polymer micelles via photocleavage of their pyrenylmethyl, *o*-nitrobenzyl, or (diethylamino)-methylcoumarinyl groups. Stupp and coworkers[33,34] described the conversion of quadruple helix of polypeptides to single fibers via photocleavage of *o*-nitrobenzyl groups.

The multiple stimuli response of a polymer that combines the light response with pH or thermosensitivity exhibited various tunable properties.[35–37] These multiple-response behaviors are very commonly seen in nature. For example, the natural rhodopsin is a photosensitive protein, whose 11-*cis* retinal covalently binds to opsin through the acid-labile Schiff base linkage. The primary event of visual perception is the conversion of its 11-*cis* retinal chromophore to the all-*trans* form on exposure to light. This light-induced isomerization effectively drives the cleavage of the acid-labile Schiff base linkage.[38–41]

Inspired by these characters, our group[42] recently proposed a preliminary protocol of a photosensitive polymer whose cinnamyl chromophores were directly linked with the acid-labile cyclic acetal linkages. Photoisomerization of cinnamyl did not only change the segmental mobility and extinction coefficient of this polymer but also deactivated the acid sensitivity of their neighboring cyclic acetal linkages. However, this deactivation was restricted by the limited *Z*-isomerization equilibrium. From both the academic and application

Additional Supporting Information may be found in the online version of this article.

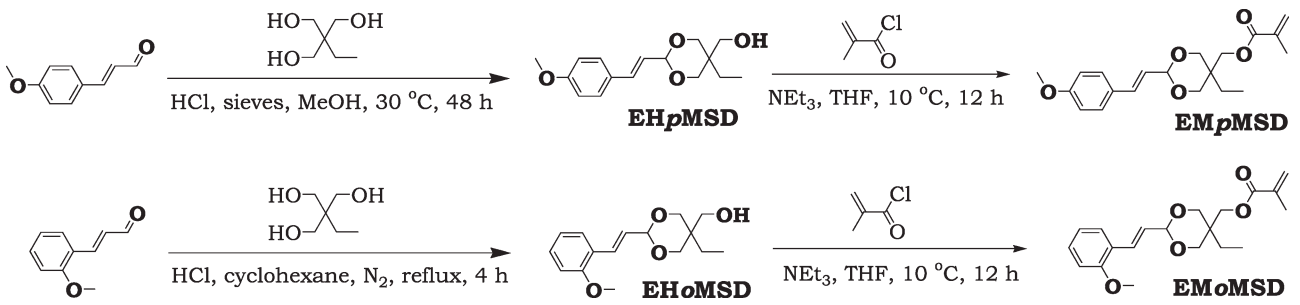

SCHEME 1 Synthesis of EM*p*MSD and EM*o*MSD monomers.

points of view, further optimization of this protocol toward the wide light tunability and effective response like the natural rhodopsin is desirable.

The cyclic acetal linkage was successfully used for the acid-cleavable polymers.[43–46] Moreover, Fréchet and coworkers[47–49] introduced the electron-donating methoxy in cyclic benzylidene acetals to activate the acid sensitivity. Colson[50] and Zhong[51] used the trimethoxy substitution of cyclic benzylidene acetals for pH-responsive expansile nanoparticles. More importantly, the methoxy substitution of cinnamyl could effectively change the equilibrium of *Z*-isomerization.[52–54] The steric hindrance of *ortho*-methoxy substitution in cinnamyl effectively lowered down the torsional barriers.[55,56]

Accordingly, we expect that introducing a methoxy in the different position of aromatic rings of cinnamyl groups will change the light-induced *Z*-isomerization thus tune the acid sensitivity of their neighboring cyclic acetal linkages of our previous prococol. This article describes our effort of the structure optimization for broadening the light-tunable acid sensitivity. To this end, the well-defined poly(5-ethyl-5-methacryloyloxy-methyl-2-(*p*-methoxystyryl)-[1,3]dioxane) (PEM*p*MSD) and poly(5-ethyl-5-methacryloyloxy-methyl-2- (*o*-methoxystyryl)-[1,3] dioxane) (PEM*o*MSD) as well as the control sample of poly(5-ethyl-5-methacryl-oyloxymethyl-2-styryl-[1,3]dioxane) (PEMSD) were synthesized via reversible addition-fragmentation chain transfer (RAFT) process. The effect of methoxy position on photoinduced *Z*-isomerization was studied by ^{1}H NMR analysis. The hydrolysis of polymers at various degrees of *Z*-isomerization was monitored by UV–vis spectroscopy and ^{1}H NMR studies. The hydrolysis of cyclic acetal linkages adjacent to either *E*-type units or *Z*-type units was separately assessed by ^{1}H NMR studies.

RESULTS AND DISCUSSION

Synthesis and Characterization of EM*p*MSD and EM*o*MSD Monomers

As shown in Scheme 1, the hydroxyl compounds, 5-ethyl-5-hydroxymethyl-2-(*o*-methoxystyryl)-[1,3]dioxane (EH*o*MSD) and 5-ethyl-5-hydroxymethyl-2-(*p*-methoxystyryl)-[1,3]dioxane (EH*p*MSD) were selected as precursors of the targeted monomers. EH*o*MSD was synthesized via condensation in refluxing cyclohexane at 95 °C, and EH*p*MSD was synthesized via condensation in anhydrous methanol at 25 °C, according to the literature precedures.[43–51] ^{1}H NMR studies confirmed the pure EH*p*MSD and EH*o*MSD compounds (Supporting Information Fig. S1).

EM*p*MSD or EM*o*MSD monomers were synthesized via esterifying EH*p*MSD or EH*o*MSD using methacryloyl chloride. As shown in Figure 1, the integral ratio of the assigned proton signals was in good agreement with the molar ratio of protons of EM*p*MSD or EM*o*MSD. Moreover, except for the signal of $CHCl_3$ impurity in $CDCl_3$, no other impurities were

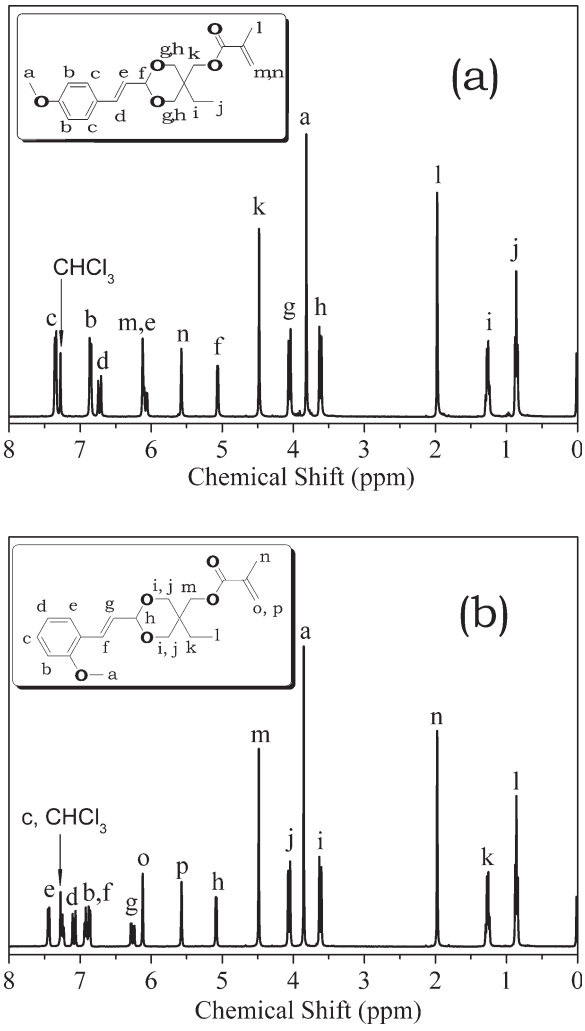

FIGURE 1 ^{1}H NMR spectra of (a) EM*p*MSD and (b) EM*o*MSD in $CDCl_3$.

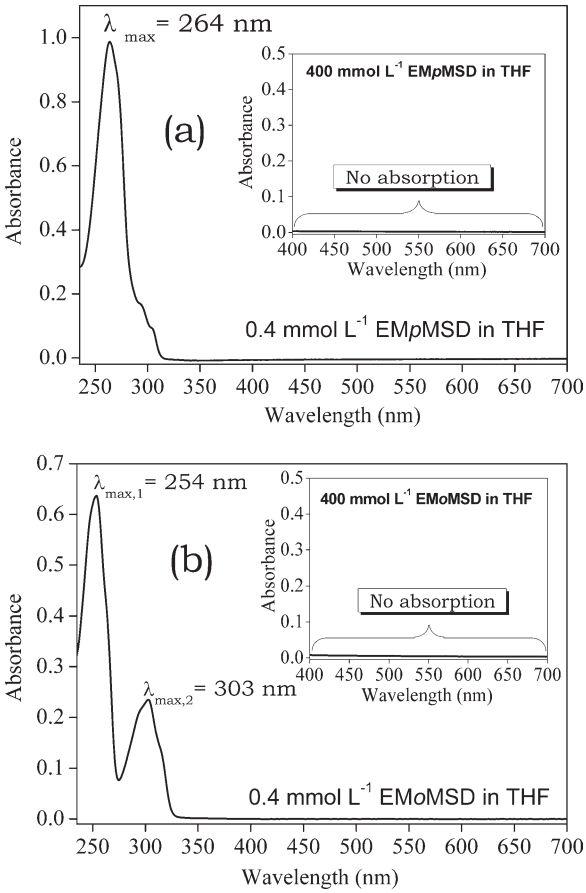

FIGURE 2 UV–vis spectra of 0.4 mmol L^{-1} of THF solution of (a) EM*p*MSD and (b) EM*o*MSD. Inset: 400 mmol L^{-1} of EM*p*MSD (a) or EM*o*MSD (b).

detectable. This suggested the high purity of monomers. Moreover, as shown in Figure 1(a), the integral ratio of I_d:I_{m+e}:I_n = 1:2:1 suggested the all *E*-type *p*-methoxy-substituted cinnamyl groups of EM*p*MSD monomer.[57] As shown in Figure 1(b), the integral ratio of I_d:I_{b+f}:I_g = 1:2:1 suggested the all *E*-type *o*-methoxy-substituted cinnamyl groups of EM*o*MSD monomer.[57]

As shown in Figure 2, the EM*p*MSD or EM*o*MSD solution exhibited a strong UV absorption at $\lambda < 350$ nm. UV light at $I_{365\ nm} = 600\ \mu W\ cm^{-2}$ could trigger *Z*-isomerization of these methoxy-substituted cinnamyl groups. However, no visible light absorption was detectable. This provided the possibility for these monomers to polymerize via RAFT process under visible light radiation at 25 °C.[58]

RAFT Polymerization of EM*p*MSD Monomer Under Visible Light Radiation at 25 °C

The visible light at mild intensity of $I_{420\ nm} = 150\ \mu W\ cm^{-2}$ was used for activating this RAFT process; this polymerization proceeded at 25 °C, using 2-cyanoprop-2-yl(4-fluoro)dithiobenzoate (CPFDB) as a chain transfer agent and (2,4,6-trimethylbenzoyl) diphenyl-phosphine oxide (TPO) as a photoinitiator (Scheme 2).

As shown in Figure 3(a), at the feed molar ratio of $[EMpMSD]_0$:$[CPFDB]_0$:$[TPO]_0$ = 100:1:0.2 in 35 wt% THF, the semilogarithmic kinetic curve linearly evolved with radiation time up to 68% monomer conversions, suggesting the constant and steady concentration of propagating radicals. Moreover, as compared to the control monomer of 5-ethyl-5-methacryloyloxymethyl-2-styryl-[1,3]dioxane (EMSD), the *para*-methoxy substitution of EM*p*MSD monomer led to the shortened initialization period,[59,60] and accelerated chain propagating in RAFT process, as indicated by the slope increase of semilogarithmic curve. The GPC traces were reasonably unimodal and symmetrical and gradually shifted to the higher molecular weight side [Fig. 3(b)]. This suggested the well-controlled behavior of this RAFT polymerization.

As shown in Figure 4(a), increasing $[EMpMSD]_0$:$[CPFDB]_0$:$[TPO]_0$ led to the shortened initialization period and accelerated chain propagating. These results were observed in the visible light-activating ambient RAFT process of glycidyl methacrylate[61] or *N*-(2-methacryloyloxyethyl)pyrrolidone.[62] At $[EMpMSD]_0$:$[CPFDB]_0$:$[TPO]_0$ = 50:1:0.2 or 100:1:0.2, the semilogarithmic kinetic curve linearly evolved. However, increasing this feed molar ratio up to 150:1:0.2 or 200:1:0.2 led to the negative deviation at relatively high conversions, presumably because of the rapid viscosity increase as suggested by slowing down of stirring bar and the broadened GPC traces (Supporting Information Fig. S2).

As shown in Figure 4b, the number-average molecular weight (M_n) linearly increased with monomer conversions

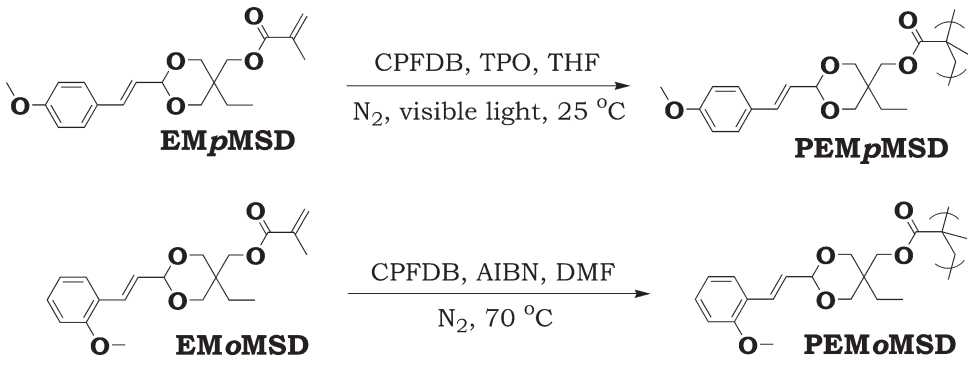

SCHEME 2 RAFT polymerization of EM*p*MSD and EM*o*MSD monomers.

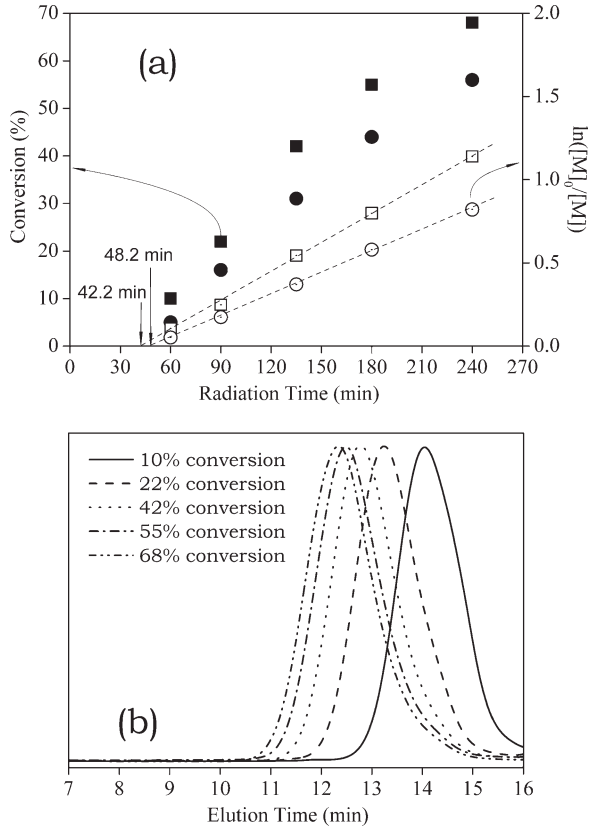

FIGURE 3 (a) Kinetic curves of RAFT polymerization of (■) EM*p*MSD or (•) EMSD using CPFDB chain transfer agent and TPO photoinitiator at [monomer]$_0$:[CPFDB]$_0$:[TPO]$_0$ = 100:1:0.2 in 35 wt% THF on irradiation with the mild visible light at $I_{420\ nm}$ = 150 μW cm^{-2} at 25 °C; (b) GPC trace evolution of PEM*p*MSD under aforementioned conditions.

over [EM*p*MSD]$_0$:[CPFDB]$_0$:[TPO]$_0$ ranging from 50:1:0.2 to 200:1:0.2. This indicated the controlled behavior of this RAFT polymerization. Clearly, these M_n values were overestimated by GPC analysis, presumably because of calibration error caused by using polystyrene standards. Thus, M_n values of the polymers for the light-tunable acid-sensitivity studies were evaluated by ^{1}H NMR studies and calculated according to the CPFDB chain ends [see inset of Fig. 5(a–c)].

EM*o*MSD polymerized very slowly in the aforementioned RAFT process because of the poor solubility in THF, DMF, or other commonly used solvents at 25 °C. To ensure homogeneous solution, this monomer was polymerized at [EM*o*MSD]$_0$:[CPFDB]$_0$:[AIBN]$_0$ = 100:1:0.3 in 80 wt% DMF and at the elevated solution temperature of 70 °C. Based on ^{1}H NMR studies, 42.5% EM*o*MSD monomer was polymerized in 4 h.

The samples of PEM*p*MSD and PEM*o*MSD with narrow distributions and similar short chain lengths of degree of polymerization (DP) ≈ 40 were selected for the light-tunable acid-sensitivity studies (Table 1). As the control sample, a well-defined PEMSD was also synthesized via RAFT polymerization using CPFDB chain transfer agent and TPO photoinitiator under visible light radiation at 25 °C.

As shown in Figure 5(a–c), no signal at δ = 5.56 ppm (one of $\underline{CH_2}$=CCH$_3$ of monomers) was detectable, suggesting the complete removal of monomers. More importantly, the integral ratios of assigned proton were in good agreement with the molar ratios of protons of the targeted polymers. This suggested the intact molecular structures of these polymers. In addition, the equal integral of d, e, and f signals for PEM*p*MSD [Fig. 5(a)], I_{d+b+f}:I_g:I_h = 3:1:1 for PEM*o*MSD [Fig. 5(b)], and the equal integral of b, c, and d signals for PEMSD [Fig. 5(c)] suggested the all *E*-type chromophores in these polymers.[57]

^{1}H NMR Evidence for the Effect of Methoxy Position on Light-Induced *Z*-isomerization

On irradiation of PEM*p*MSD solution with the full-wave UV light at $I_{365\ nm}$ = 600 μW cm^{-2} in N$_2$ gas atmosphere at 25 °C [Fig. 6(a)], the signal at δ = 6.0 ppm (*E*-type *p*-CH$_3$OC$_6$H$_4$CH=$\underline{CH}$) attenuated. A new signal at δ = 5.6 ppm (*Z*-type *p*-CH$_3$OC$_6$H$_4$CH=$\underline{CH}$) appeared, and the signal at δ = 4.9 ppm (O$\underline{CH}$O of cyclic acetal linkages) shifted to the low field. This suggested the *Z*-isomerization of the *p*-methoxy-substituted cinnamyl groups.

The integral of signal O$\underline{CH}$O was equal to the total integrals of *E*-type and *Z*-type signals *p*-CH$_3$OC$_6$H$_4$CH=$\underline{CH}$ after

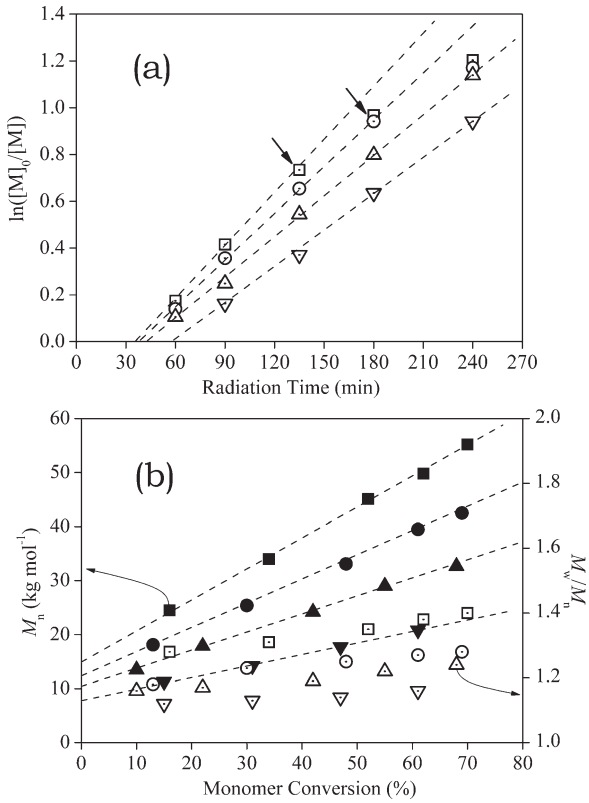

FIGURE 4 (a) Kinetic curves and (b) the evolution of number-average molecular weight (M_n, solid) and polydispersity index (M_w/M_n, hollow) in RAFT polymerization of EM*p*MSD using CPFDB chain transfer agent and TPO photoinitiator at [EM*p*MSD]$_0$:[CPFDB]$_0$:[TPO]$_0$ of (■) 200:1:0.2, (•) 150:1:0.2, (▲) 100:1:0.2, (▼) 50:1:0.2 in 35 wt% THF under visible light radiation at $I_{420\ nm}$ =150 μW cm^{-2} at 25 °C.

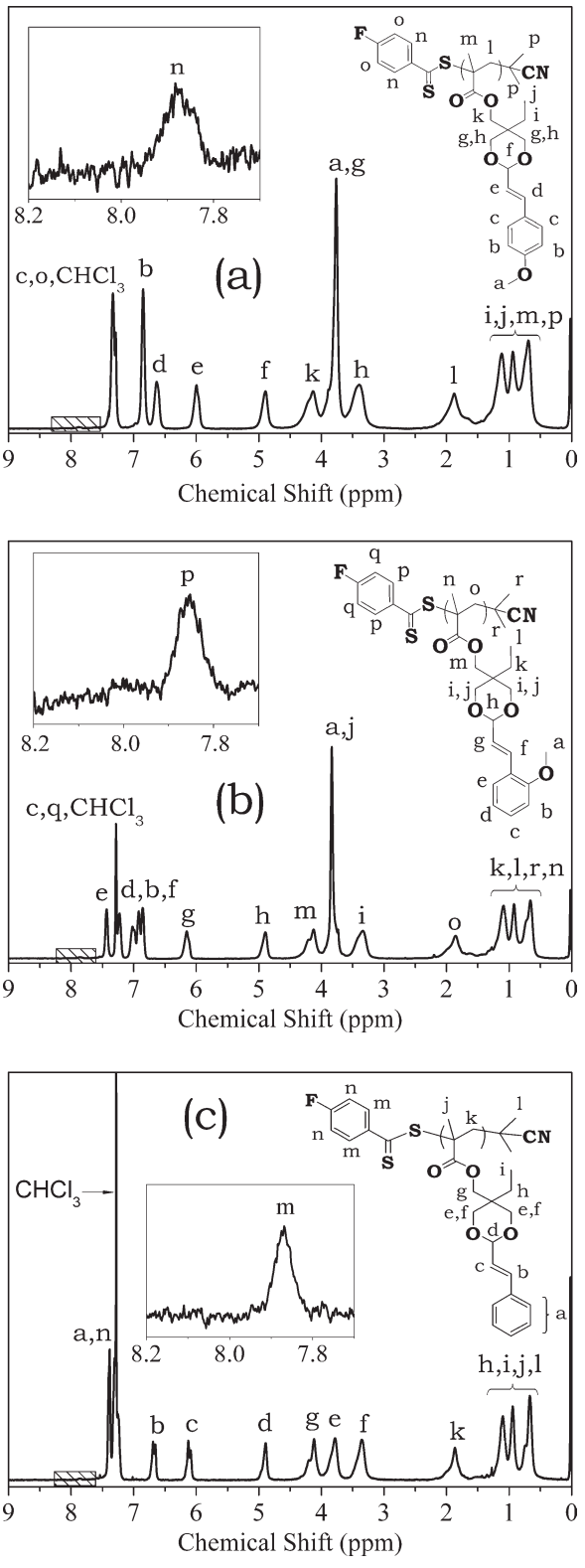

FIGURE 5 ^{1}H NMR spectra of the $CDCl_3$ solutions of (a) PEM*p*MSD, (b) PEM*o*MSD, and (c) PEMSD that were used for the light-tunable acid-sensitivity studies.

irradiation for 12 h. This suggested that only *Z*-isomerization occurred, that is, [2+2] photocycloaddition that occurred irreversibly in the polymeric cinnamic ester moieties[63–66] or reversibly in the polymeric coumarin moieties[67,68] was negligible. In addition, this *Z*-isomerization was a typical equilibrium reaction, similar to their small-molecular analogs.[69]

In contrast, as shown in Figure 6(b), the *ortho*-methoxy substitution in PEM*o*MSD led to the rapid attenuation of signal at δ = 6.15 ppm (*E*-type *o*-$CH_3OC_6H_4CH{=}C\underline{H}$) and rapid increase of new signal at δ = 5.67 ppm (*Z*-type *o*-$CH_3OC_6H_4CH{=}C\underline{H}$). The new signal of *Z*-type *o*-$CH_3OC_6H_4CH{=}C\underline{H}$ was remarkably larger than that of *E*-type one after irradiation for 12 h, suggesting the significant shift of this equilibrium to *Z*-type. In addition, the total integral of *E*- and *Z*-type *o*-$CH_3OC_6H_4CH{=}C\underline{H}$ was equal to that of O$C\underline{H}$O. This suggested the negligible [2+2] cycloaddition or other side reactions. However, the GPC traces were slightly broadened after irradiation for 12 h (Supporting Information Fig. S3), presumably because of the side reaction induced by the photolysis of CTA chain ends. Further studies are necessary to clarify this phenomenon but beyond the scope of this article.

The degrees of *Z*-isomerization of PEM*p*MSD, PEM*o*MSD, and PEMSD were precisely assessed by ^{1}H NMR studies (see Supporting Information). As shown in Figure 7, PEM*p*MSD exhibited the *Z*-isomerization kinetics comparable to the nonsubstituted PEMSD, with the equilibrium degree of *Z*-isomerization of 66%, slightly higher than 62% of PEMSD. The photoisomerization of PEM*o*MSD reached the equilibrium of 81% *Z*-type. This suggested that the *ortho*-methoxy substitution favored the *Z*-type formation.

UV–vis Spectroscopic Evidence for the Effect of Methoxy Position on Light-Tunable Acid Sensitivity

After adding the catalytic amount of hydrochloric acid in the all *E*-type PEM*p*MSD solution at 25 °C [Fig. 8(a)], the absorbance of a new peak of *p*-methoxyphenylacrylaldehyde at λ_{max} = 315 nm increased rapidly, suggesting the rapid hydrolysis. However, this absorbance increased much more slowly than the former for the 61% *Z*-isomerized PEM*p*MSD sample [Fig. 8(b)], suggesting that *Z*-isomerization deactivated this hydrolysis. Similarly, *Z*-isomerization of PEM*o*MSD (Supporting Information Fig. S4) or PEMSD (Supporting Information Fig. S5) also slowed down this hydrolysis. This suggested that the *Z*-type groups prevented their neighboring cyclic acetal linkages from hydrolysis.

The degree of hydrolysis was assessed according to Lambert–Beer law (see Supporting Information Fig. S6). As shown in Figure 9(a), PEM*p*MSD was completely hydrolyzed in shortly ~60 min because of the electron-donating effect caused by the *para*-methoxy substitution,[47,70] which was quite shorter than ~540 min needed for the complete hydrolysis of PEMSD. While the *ortho*-methoxy substitution of PEM*o*MSD slowed down this hydrolysis, which was essentially complete in moderately ~180 min. Moreover, *Z*-isomerization remarkably deactivated this hydrolysis [Fig. 9(b)]. After 1800 min, the 62% *Z*-type PEM*o*MSD sample hydrolyzed 46%, similar to

TABLE 1 Monomer Conversions Controlled in RAFT Processes and Molecular Structure Parameters of PEM*p*MSD, PEM*o*MSD, and PEMSD that were Selected for Light-Tunable Acid-Sensitivity Studies

Sample	Monomer Conversion[a] (%)	$M_{n,GPC}$ (kg mol^{-1})	M_w/M_n	$M_{n,NMR}$ (kg mol^{-1})	DP[a]
PEM*p*MSD	40.2	21.2	1.18	13.7	39
PEM*o*MSD	42.5	22.9	1.19	14.4	41
PEMSD	43.8	20.9	1.16	13.8	43

[a] The monomer conversions and DP were assessed by ^{1}H NMR studies.

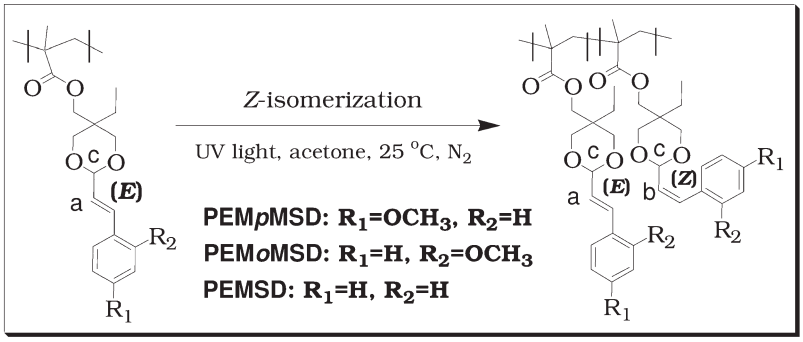

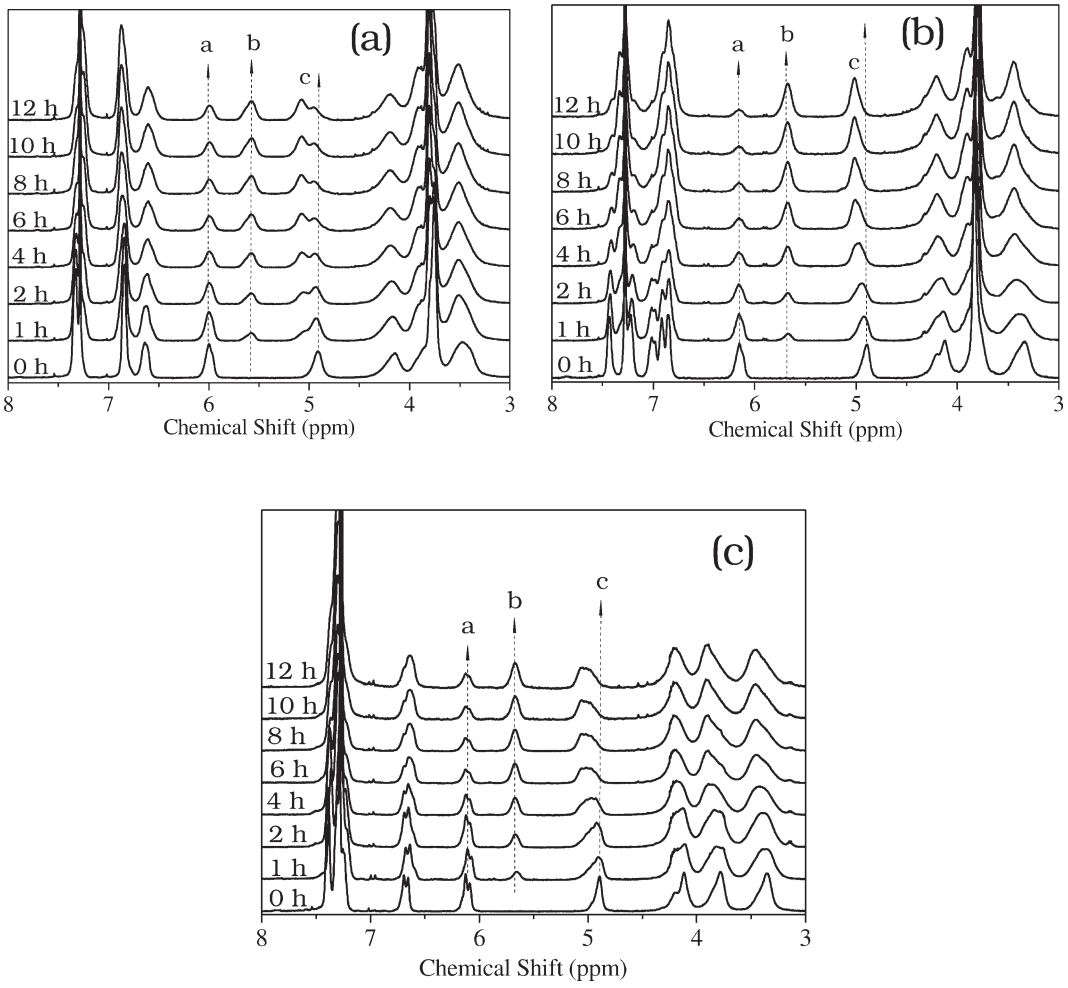

FIGURE 6 The evolution of ^{1}H NMR spectrum of 5.0 mg mL^{-1} PEM*p*MSD (a), PEM*o*MSD (b), or PEMSD (c) on irradiation with full-wave UV light of mercury lamp at $I_{365\ nm} = 600\ \mu W\ cm^{-2}$ in nitrogen gas atmosphere at 25 °C.

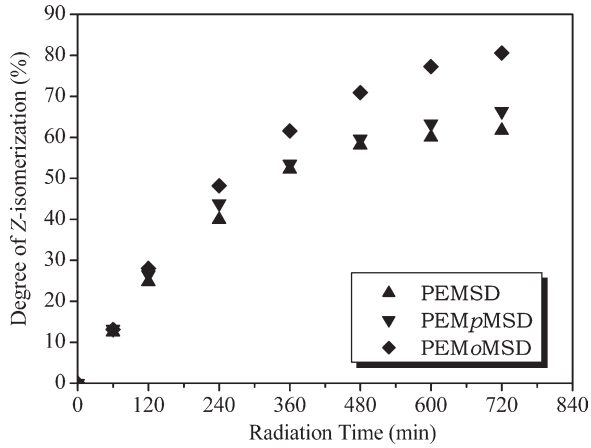

FIGURE 7 The evolution of degrees of *Z*-isomerization of the 100% *E*-type PEMSD, PEM*p*MSD, and PEM*o*MSD on irradiation with full-wave UV light of mercury lamp at $I_{365\ nm} = 600\ \mu W\ cm^{-2}$ in nitrogen gas atmosphere at 25 °C.

37% hydrolysis of the 60% *Z*-type PEMSD sample, while the 61% *Z*-type PEM*p*MSD sample hydrolyzed up to 91%.

^{1}H NMR Evidence for the Effect of Methoxy Position on Light-Tunable Acid Sensitivity

^{1}H NMR was used to precisely evaluate this light-tunable acid sensitivity. Both the all *E*-type and 61% *Z*-type PEM*p*MSD samples were separately dissolved in acetone-d_6 with the addition of catalytic amount of deuterated hydrochloric acid at 25 °C. ^{1}H NMR spectra were recorded at the predetermined intervals.

As shown in Figure 10(a), after adding hydrochloric acid in the all *E*-type PEM*p*MSD solution at 25 °C in shortly 10 min, the signals of *p*-methoxyphenylacrylaldehyde at $\delta = 9.64$, 7.69, and 7.03 ppm appeared, indicating the hydrolysis of cyclic acetal linkages. In contrast, for the 61% *Z*-isomerized PEM*p*MSD solution [Fig. 10(b)], *p*-$CH_3OC_6H_4CH{=}C\underline{H}$ signal of *Z*-type units attenuated much more slowly than that of *E*-type units. Moreover, the higher field signal at $\delta = 5.00$ ppm (OC$\underline{H}$O of *E*-type units) attenuated rapidly and disappeared in shortly 66 min, while the lower field signal of OC$\underline{H}$O of *Z*-type units at $\delta = 5.13$ ppm was still detectable after hydrolyzing for 536 min. This suggested that the *Z*-type units hydrolyzed more slowly than *E*-type units.

In contrast, for the all *E*-type PEM*o*MSD solution [Fig. 11(a)], the signals at $\delta = 6.20$ ppm (*o*-$CH_3OC_6H_4CH{=}C\underline{H}$) and at $\delta = 5.03$ ppm (OC$\underline{H}$O) attenuated much more slowly than those from the all *E*-type PEM*p*MSD [Fig. 10(a)], which were still detectable in 168 min. More importantly, for the 81% *Z*-isomerized PEM*o*MSD sample [Fig. 11(b)], the signal of *E*-type *o*-$CH_3OC_6H_4CH{=}C\underline{H}$ disappeared in 535 min, and the signal of *Z*-type *o*-$CH_3O\underline{C}_6H_4CH{=}C\underline{H}$ was still very strong. This evidenced that this *Z*-isomerization improved the stability of cyclic acetal linkages against hydrolysis.

The ^{1}H NMR assessment of degree of hydrolysis from either *E*-type or *Z*-type units was described in Supporting Information. As shown in Figure 12(a), the all *E*-type PEM*p*MSD hydrolyzed more rapidly than the all *E*-type PEMSD [Fig. 13(a)], which was essentially complete in 65 min. Moreover, the partially *Z*-isomerized PEM*p*MSD hydrolyzed rapidly at the early stage and slowed down after *E*-type units were completely hydrolyzed [Fig. 12(b)]. Their *E*-type units hydrolyzed at the comparable rate to the all *E*-type PEM*p*MSD [Fig. 12(a)]. Meanwhile, their *Z*-type units hydrolyzed at the comparable rate at different degrees of *Z*-isomerization, more rapidly than *Z*-type units in PEMSD samples [Fig. 13(b)] but slower than their corresponding *E*-type units over the range of [*E*]:[*Z*]=72:28–39:61.

As shown in Figure 14(a), as varying the configuration from 100% *E*-type to 81% *Z*-type, the degree of hydrolysis of PEM*o*MSD samples changed from 100% to 33% in 570 min, implying the remarkable light-tunability of acid sensitivity. As shown in Figure 14(b), the hydrolysis of *E*-type units was accelerated, but the hydrolysis of *Z*-type units was slowed

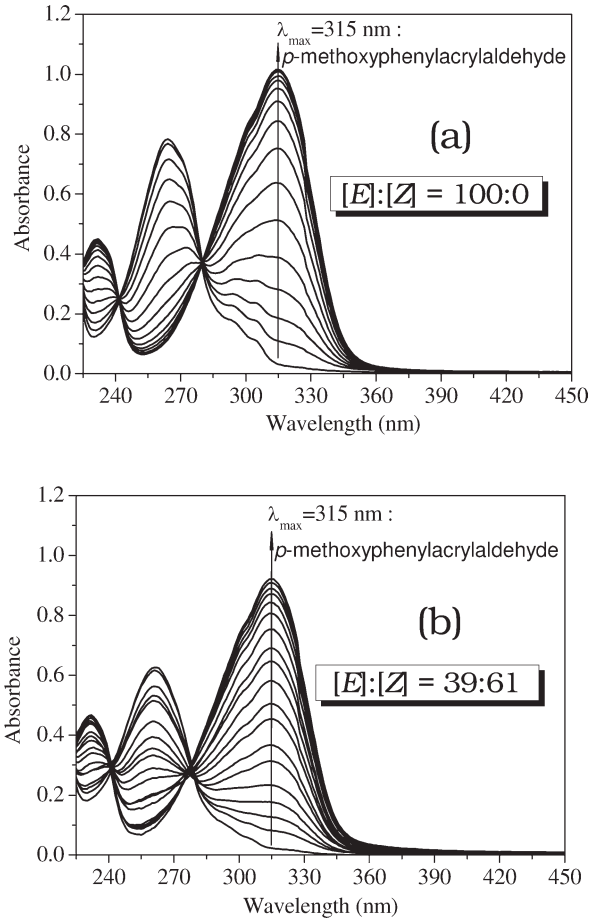

FIGURE 8 UV–vis spectra of 1,4-dioxane solutions of PEM*p*MSD at [*E*]:[*Z*] = 100:0 (a) or 39:61 (b), hydrolyzed under the conditions: 0.25 g of 0.98 mol L^{-1} HCl solution was added in 50 mL of 12.0 mg L^{-1} PEM*p*MSD solution, stirred at 25 °C for the predetermined intervals. (a) From bottom to upper: 0, 5, 10, 15, 20, 25, 30, 35, 40, 45, 50, 55, 60, 70, 80, 90, 100, 110, and 120 min; (b) from bottom to upper: 0, 15 30, 45, 60, 90, 120, 180, 240, 360, 480, 600, 720, 900, 1080, 1260, 1440, 1620, and 1800 min.

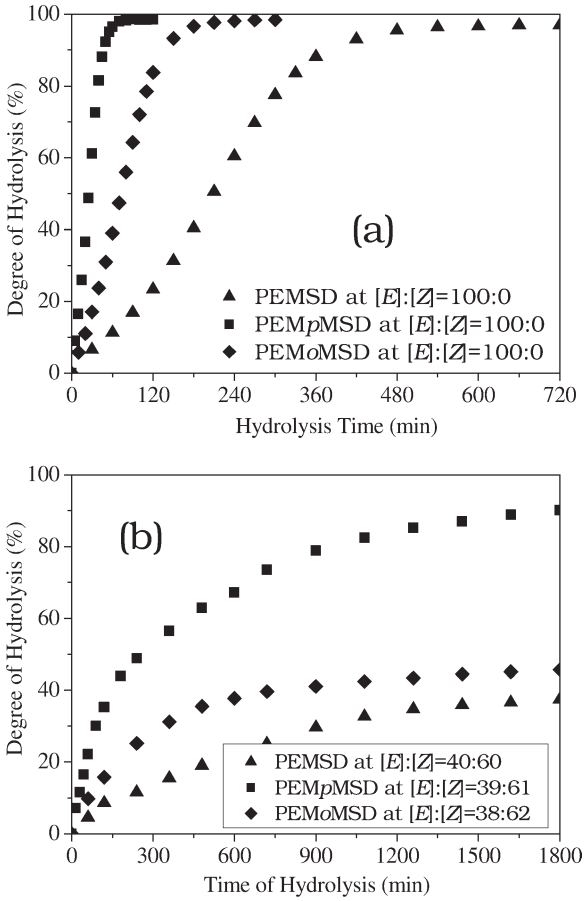

FIGURE 9 The hydrolysis kinetic curves of PEMSD, PEM*p*MSD, and PEM*o*MSD monitored by UV–vis spectrophotometry under the conditions described in Figure 8: (a) 100% *E*-type polymers, (b) approximately 60% *Z*-type polymers.

down. Only 24% of *Z*-type units hydrolyzed in 570 min, close to 22% hydrolysis of *Z*-type EMSD units in 540 min. This indicated that this isomerization-induced deactivation of hydrolysis was enough to neutralize the activation caused by the electron-donating *o*-methoxy substitution.

As far as the chemical mechanism was concerned, this light-tunable hydrolysis was quite similar to the cleavage of the Schiff base linkage of rhodopsin on exposure to light.[38–41] Moreover, adjusting the position of a single methoxy in aromatic rings of cinnamyl groups widely changed the light-tunable acid sensitivity of their neighboring cyclic acetal linkages. This intriguing strategy may be essential in the molecular design of novel polymers for photosensors and light-tuned drug delivery.

EXPERIMENTAL

Materials

EMSD was synthesized according to our previous procedures.[42] CPFDB was synthesized according to the literature procedures.[71] 2,2′-Azobis(isobutyronitrile) (AIBN, 98%; Aldrich), *p*-methoxyphenylacrylaldehyde, and *o*-methoxyphenylacrylaldehyde (95%, Yuancheng Reagent Co.) were recrystallized from ethanol at −20 °C and dried in vacuo at 30 °C. TPO (97%; Runtec Chem. Co.), 2-ethyl-2-hydroxymethyl-1,3-propane-diol (98%; Aldrich), and methacrylic chloride (97%; Aldrich) were used as received. $CDCl_3$, acetone-d_6, and deuterated hydrochloric acid were purchased from Cambridge Isotope Laboratory, and used as received. DMF, THF, 1,4-dioxane, and triethylamine were dried over metallic sodium, distilled prior to use. Methanol and ethyl ether were dried over metallic magnesium and distilled prior to use. Acetone was treated with K_2MnO_4 and anhydrous $MgSO_4$ and distilled prior to use. Chloroform was washed with distilled water, dried over anhydrous $CaCl_2$ overnight, and distilled prior to use.

Visible Light Used for Activating RAFT Polymerization at 25 °C

A mercury vapor lamp emitting separately at 254, 302, 313, 365, 405, 436, 545, and 577 nm was selected. JB400 filters were used to filter out the shorter-wave UV light at $\lambda < 400$ nm and adjust the light intensity. The light intensity was measured using a UV-A radiometer that was equipped with a 420-nm sensor. Thus the visible light emitting at 405, 436, 545, and 577 nm at mild intensity of $I_{420\ nm} = 150\ \mu W\ cm^{-2}$ was obtained for this purpose.

Synthesis of EH*p*MSD

p-Methoxyphenylacrylaldehyde (32.40 g, 0.20 mol) and 2-ethyl-2-hydroxymethyl-1,3-propanediol (32.16 g, 0.24 mol) were dissolved in 250 mL of anhydrous methanol in a 500 mL round-bottom flask. In this flask, 0.5 mL of 8.0 mol L^{-1} hydrochloric acid and 64 g dried 4 Å molecular sieves were added. The mixture was stirred at 25 °C for 48 h. Triethylamine (2 mL) was added to neutralize this solution. The mixture was filtrated, and methanol was removed by rotary evaporation and dissolved in 200 mL chloroform. The solution was washed using 2 wt% Na_2CO_3, saturated NaCl solution, and distilled water until it was neutralized. The solution was dried over anhydrous $MgSO_4$ overnight. After filtration, chloroform was removed by rotary evaporation. The crude product was recrystallized from ethyl ether at −20 °C, dried in vacuo overnight to afford white solid product.

Weight: 31.25 g; yield: 56%. ^{1}H NMR (δ, in $CDCl_3$, ppm): 0.88 (3H, CCH_2CH_3), 1.24 (2H, CCH_2CH_3), 3.61 (2H, two protons of OCH_2CCH_2O), 3.82 (3H, $C_6H_4OCH_3$), 3.95 (2H, CH_2OH), 4.05 (2H, two protons of OCH_2CCH_2O), 5.07 (1H, OCHO), 6.10 (1H, $C_6H_4CH{=}CH$), 6.72 (1H, $C_6H_4CH{=}CH$), 6.87 (2H, 2 protons of $C_6H_4CH{=}CH$), 7.36 (2H, two protons of $C_6H_4CH{=}CH$).

Synthesis of EH*o*MSD

2-Ethyl-2-hydroxymethyl-1,3-propanediol (32.16 g, 0.24 mol), *o*-methoxyphenylacryl-aldehyde (32.40 g, 0.20 mol), 150 mL cyclohexane, and 0.5 mL of 8.0 mol L^{-1} hydrochloric acid were charged in a 500 mL round-bottom flask that was equipped with a water separator. The solution was refluxed at 95 °C for 4 h. Water was removed by azeotropic distillation. The solution was cooled down to 25 °C. The oil phase was separated and washed subsequently using 2 wt% Na_2CO_3, the saturated solution of NaCl, and distilled water

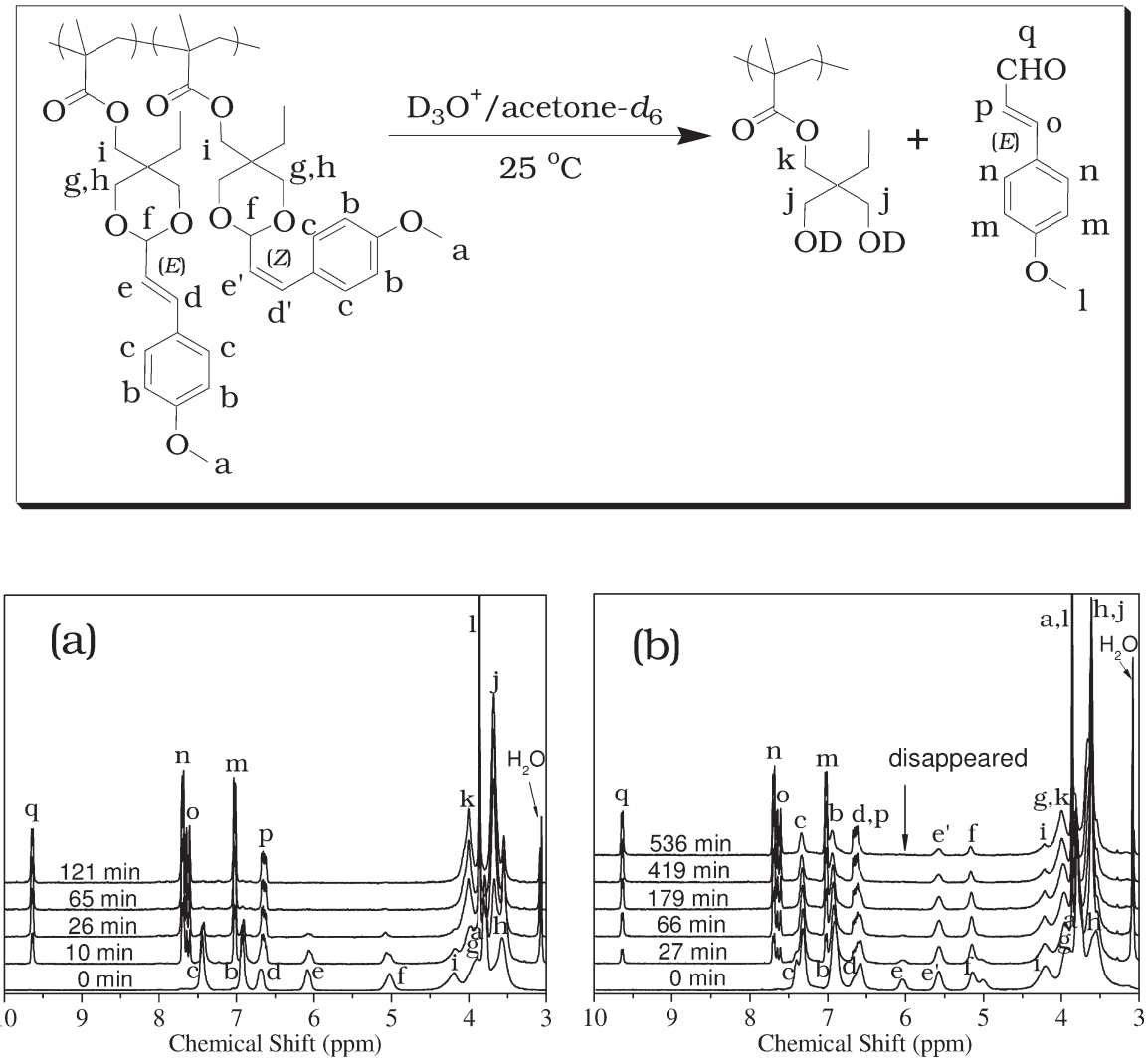

FIGURE 10 The evolution of ^{1}H NMR spectrum of PEM*p*MSD at [*E*]:[*Z*] = 100:0 (a) or 39:61 (b) on hydrolyzing in 1.0 mL of 6.0 mg mL^{-1} acetone-d_6 solution with the addition of 13 mg of 0.25 mol L^{-1} deuterated hydrochloric acid at 25 °C.

until it was neutralized. This solution was dried over anhydrous $MgSO_4$ overnight. After filtration, the solvent was removed by rotary evaporation. The crude product was purified through silica column using the mixed petroleum ether and ethyl acetate eluent (3:1, v/v), recrystallized from ethyl ether at −20 °C, and dried in vacuo overnight to afford white solid product.

Weight: 22.82 g; yield: 41%. ^{1}H NMR (δ, in $CDCl_3$, ppm): 0.88 (3H, $CCH_2C\underline{H}_3$), 1.24 (2H, $CC\underline{H}_2CH_3$), 3.58 (2H, two protons of $OC\underline{H}_2C\underline{C}H_2O$), 3.82 (3H, $C_6H_4OC\underline{H}_3$), 3.96 (2H, $C\underline{H}_2OH$), 4.03 (2H, two protons of $OC\underline{H}_2C\underline{C}H_2O$), 5.07 (1H, $O\underline{C}HO$), 6.28 (1H, $C_6H_4CH{=}C\underline{H}$), 6.86–6.94 (2H, $C_6H_4C\underline{H}{=}CH$ and one proton of $C_6\underline{H}_4CH{=}CH$), 7.06 (1H, one proton of $C_6\underline{H}_4CH{=}CH$), 7.25 (1H, one proton of $C_6\underline{H}_4CH{=}CH$), 7.43 (1H, one proton of $C_6\underline{H}_4CH{=}CH$).

Synthesis of EM*p*MSD

EH*p*MSD (22.24 g, 0.08 mol), triethylamine (12.12 g, 0.12 mol), and 150 mL of anhydrous THF were charged in a 500 mL dried flask. The flask was immersed in a water/ice bath at 0 °C. Methacryloyl chloride (10.03 g, 96 mmol) was dissolved in 75 mL of anhydrous THF and added dropwise to this flask under stirring over 2 h. The mixture was stirred at 10 °C overnight. The white ammonium salt was filtered out. The solution was concentrated by rotary evaporation, dissolved in 150 mL ethyl ether, washed using 2 wt% Na_2CO_3, saturated NaCl solution, and distilled water until it was neutralized. The solution was dried over anhydrous $MgSO_4$. After filtration, the solvent was removed by rotary evaporation. The crude product was purified through silica column using the mixed eluent of petroleum ether and ethyl acetate (8:1, v/v), recrystallized from mixed petroleum ether and ethyl acetate eluent (3:1, v/v) at −20 °C, dried in vacuo overnight to afford white solid product.

Weight: 11.63 g; yield: 42%. ^{1}H NMR (δ, in $CDCl_3$, ppm): 0.86 (3H, $CCH_2C\underline{H}_3$), 1.25 (2H, $CC\underline{H}_2CH_3$), 1.98 (3H, $C\underline{H}_3C{=}CH_2$), 3.63 (2H, two protons of $OC\underline{H}_2C\underline{C}H_2O$), 3.82 (3H, $C_6H_4OC\underline{H}_3$), 4.07 (2H, two protons of $OC\underline{H}_2C\underline{C}H_2O$), 4.48

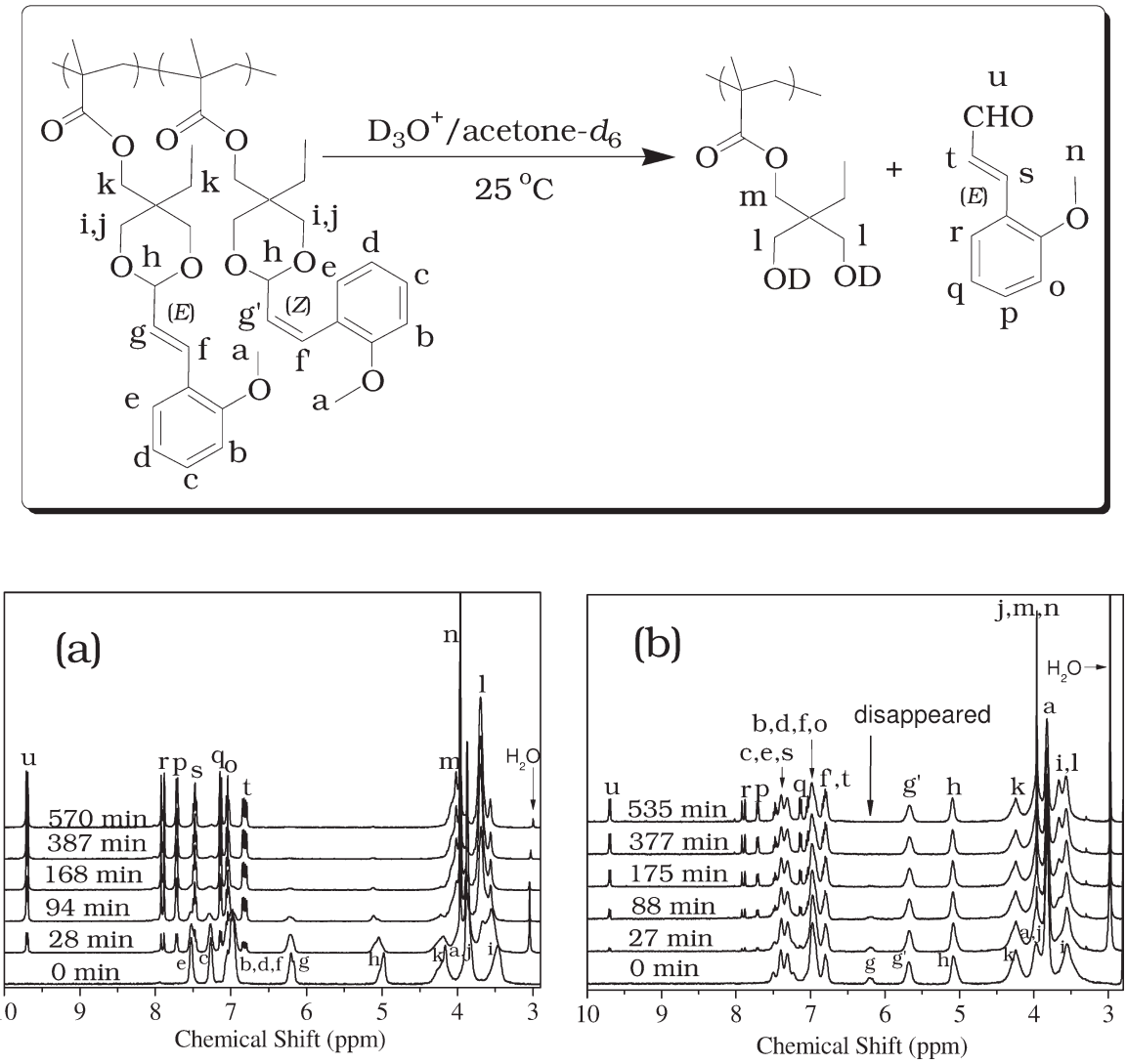

FIGURE 11 The evolution of ^{1}H NMR spectrum of PEM*o*MSD at [*E*]:[*Z*] = 100:0 (a) or 20:80 (b) on hydrolyzing in 1.0 mL of 6.0 mg mL^{-1} acetone-d_6 solution with the addition of 13 mg of 0.25 mol L^{-1} deuterated hydrochloric acid at 25 °C.

(2H, $COOCH_2$), 5.06 (1H, OCHO), 5.57 (1H, one proton of $CH_3C{=}CH_2$), 6.06 (1H, $C_6H_4CH{=}CH$), 6.12 (1H, one proton of $CH_3C{=}CH_2$), 6.75 (1H, $C_6H_4CH{=}CH$), 6.87 (2H, two protons of C_6H_4 CH=CH), 7.36 (2H, two protons of C_6H_4 CH=CH).

The synthesis of EM*o*MSD follows the same procedure except for using EH*o*MSD and eluent of petroleum ether–ethyl acetate (6:1, v/v).

Weight: 10.80 g; yield: 39%. ^{1}H NMR (δ, in $CDCl_3$, ppm): 0.86 (3H, CCH_2CH_3), 1.25 (2H, CCH_2CH_3), 1.98 (3H, $CH_3C{=}CH_2$), 3.63 (2H, 2 protons of OCH_2CCH_2O), 3.85 (3H, $C_6H_4OCH_3$), 4.05 (2H, two protons of OCH_2CCH_2O), 4.48 (2H, $COOCH_2$), 5.08 (1H, OCHO), 5.57 (1H, one proton of $CH_3C{=}CH_2$), 6.12 (1H, one proton of $CH_3C{=}CH_2$), 6.28 (1H, $C_6H_4CH{=}CH$), 6.86–6.95 (2H, $C_6H_4CH{=}CH$ and one proton of $C_6H_4CH{=}CH$), 7.06 (1H, one proton of $C_6H_4CH{=}CH$), 7.25 (1H, one proton of $C_6H_4CH{=}CH$), 7.43 (1H, one proton of $C_6H_4CH{=}CH$).

Visible Light-Activated RAFT Polymerization of EM*p*MSD Monomer at 25 °C

EM*p*MSD (3.46 g, 10.0 mmol), CPFDB (23.9 mg, 0.1 mmol), TPO (7.0 mg, 0.02 mmol), and 1.88 g of anhydrous THF were charged in a 25 mL flask and capped with rubber septa. After bubbling with nitrogen gas for 40 min, the flask was immersed in water bath at 25 °C and irradiated with visible light. Samples were collected using deoxygenated syringes at predetermined intervals and quenched by exposing to air and adding small amount of hydroquinone inhibitor. One portion of sample was diluted in $CDCl_3$ for ^{1}H NMR studies. Another portion was diluted in DMF for GPC analysis. The resultant PEM*p*MSD was precipitated from large excess of anhydrous methanol and dried in vacuo overnight. The visible light-activating RAFT polymerization of EMSD at 25 °C was the same except for using EMSD monomer.

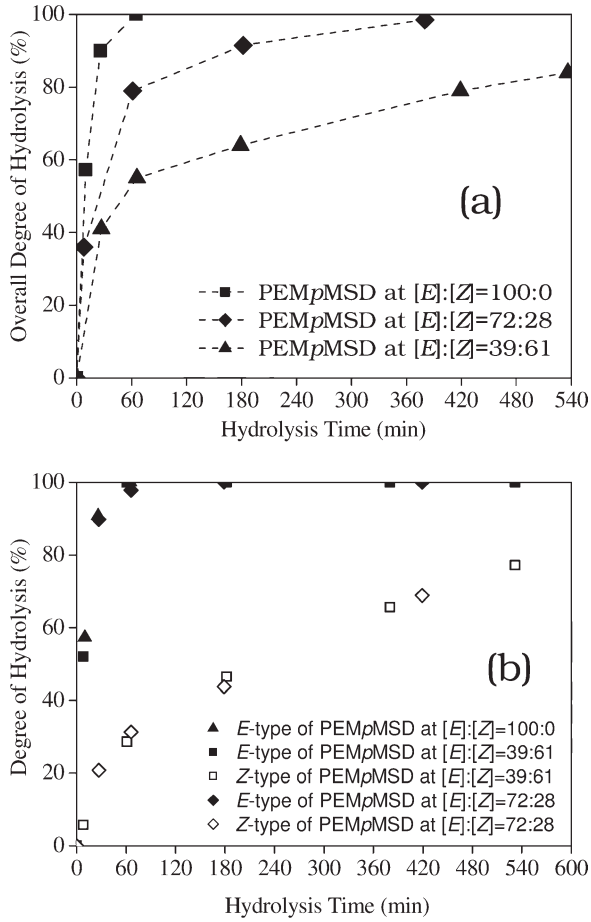

FIGURE 12 (a) The overall degree of hydrolysis of PEM*p*MSD at [*E*]:[*Z*] = 100:0, 72:28, or 39:61 as a function of hydrolysis time under the hydrolyzing conditions described in Figure 10. (b) The degrees of hydrolysis of *E*-type units (solid) or *Z*-type units (hollow) of PEM*p*MSD as mentioned above.

RAFT Polymerization of EM*o*MSD Monomer at 70 °C

EM*o*MSD (1.73 g, 5.0 mmol), CPFDB (12.0 mg, 0.05 mmol), AIBN (2.5 mg, 0.015 mmol), and anhydrous DMF (7.00 g) were charged in a 25 mL round-bottom flask and capped with rubber septa. After bubbling with nitrogen gas for 40 min, the flask was immersed in a thermostatic oil bath at 70 °C for 4 h. The solution was exposed to air by adding small amount of hydroquinone inhibitor. The resultant PEM*o*MSD was precipitated from large excess of anhydrous methanol and dried in vacuo overnight.

Photoinduced *Z*-Isomerization of PEM*p*MSD Under UV Light Radiation

The typical procedures were as follows. PEM*p*MSD (0.10 g) was dissolved in 20 mL of acetone under stirring in a 50-mL quartz flask capped with rubber septa. The solution was deoxygenated by purging with nitrogen gas for 30 min. The flask was immersed in a water bath at 25 °C and irradiated with the full-wave UV light with intensity of $I_{365\ nm} = 600\ \mu W\ cm^{-2}$. The samples were collected at the predetermined intervals. Acetone was removed under reduced pressure at 25 °C. The polymer was dissolved in $CDCl_3$ for ^1H NMR analysis. The photoisomerization of PEMSD or PEM*o*MSD was the same except for using PEMSD or PEM*o*MSD.

UV–Vis Spectroscopic Studies on Light-Tunable Acid Sensitivity of Polymers

The typical procedures were as follows. PEM*p*MSD was dissolved in 1,4-dioxane under stirring at 25 °C and diluted to 12 mg L^{-1}. A 100-mL round-bottom flask was charged with 50 mL of such solution. This flask was charged with 0.25 g of 0.98 mol L^{-1} hydrochloric acid under stirring at 25 °C. UV–vis spectra were recorded at predetermined intervals.

^1H NMR Studies on Light-Tunable Acid Sensitivity of These Polymers

The typical procedures were as follows. PEM*p*MSD (6 mg) was dissolved in 1.0 mL of acetone-d_6 in an NMR sample tube at 25 °C. This tube is charged with 13 mg of 0.25 mol L^{-1} deuterated hydrochloric acid. ^1H NMR spectra were recorded at predetermined intervals at 25 °C.

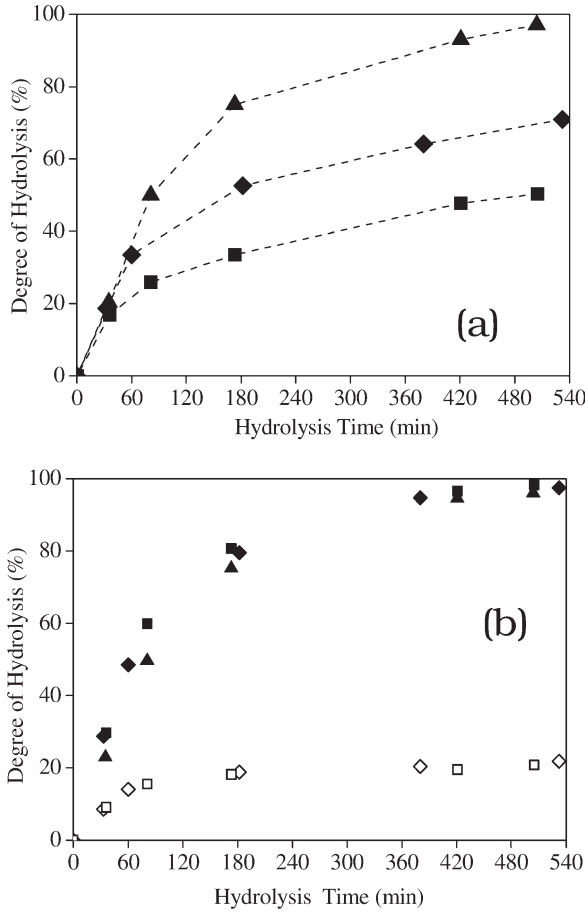

FIGURE 13 (a) The overall degree of hydrolysis of PEMSD at [*E*]:[*Z*] = 100:0 (▲), 70:30 (◆) or 40:60 (■) as a function of hydrolysis time under the hydrolyzing conditions as described in Figure 10. (b) The degrees of hydrolysis of *E*-type units (solid) or *Z*-type units (hollow) of the corresponding PEMSD as mentioned above.

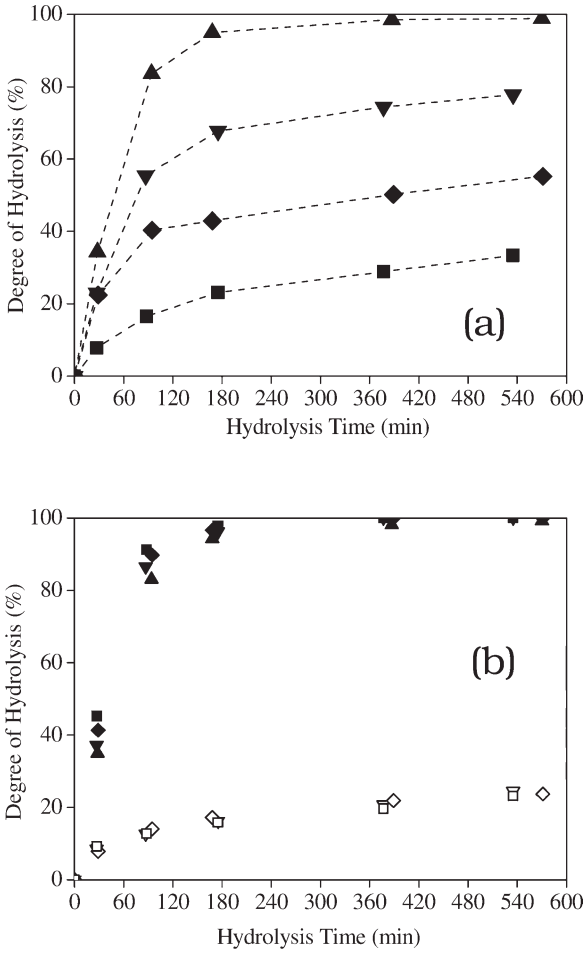

FIGURE 14 (a) The overall degree of hydrolysis of PEM*o*MSD at [*E*]:[*Z*] = 100:0 (▲), 68:32 (▼), 38:62 (◆), or 20:80 (■) as a function of hydrolysis time under the hydrolyzing conditions as described in Figure 11. (b) The degrees of hydrolysis of *E*-type units (solid) or *Z*-type units (hollow) of this PEM*o*MSD.

Analytical Techniques

GPC was performed on a PL-GPC120 setup being equipped with a column set consisting of two PL gel 5 μm MIXED-D columns (7.5 $\times$ 300 mm^2, effective molecular weight range of 0.2–400.0 kg mol^{-1}), using DMF as an eluent that contained 0.01 M LiBr at 80 °C, at a flow rate of 1.0 mL min^{-1}. Polystyrene standards over the molecular weight range of 0.5–7500.0 kg mol^{-1} (PSS, Mainz, Germany) were used for calibration. ^{1}H NMR analyses were performed on a Bruker AV-400 NMR spectrometer. Samples were scanned for 16 times at 25 °C. UV–vis spectra were recorded on a PerkinElmer Lambda 25 spectrometer at 25 °C.

CONCLUSIONS

This article described a rhodopsin-inspired photosensitive polymer whose light-tunable acid sensitivity was widely modulated simply by adjusting the position of a methoxy substituent in the aromatic rings of cinnamyl groups. The *para*- or *ortho*-methoxy-substituted EM*p*MSD and EM*o*MSD monomers as well as EMSD monomer were synthesized. EM*p*SMD and EMSD monomers were polymerized via RAFT polymerization under visible light radiation at 25 °C. EM*o*MSD monomer was polymerized via RAFT polymerization at 70 °C because of the poor solubility.

The kinetic results demonstrated that the *para*-methoxy substitution led to the shortened initialization period and accelerated chain propagation in RAFT process under visible light radiation at 25 °C. This RAFT process was well controlled at the low feed molar ratio of [EM*p*MSD]$_0$: [CPFDB]$_0$:[TPO]$_0$ = 50:1:0.2 or 100:1:0.2, and increasing this feed molar ratio led to the ill-controlled polymerization. Thus the well-defined PEM*p*MSD, PEM*o*MSD, and PEMSD samples with the similar short chain lengths of DP $\approx$ 40 were synthesized for the light-tunable acid-sensitivity studies.

^{1}H NMR studies evidenced the high degree of light-induced *Z*-isomerization of the *ortho*-methoxy-substituted PEM*o*MSD, which reached up to 81% at equilibrium. UV–vis spectroscopic studies demonstrated that the para-methoxy substitution of cinnamyl in PEMpMSD led to the rapid hydrolysis of their neighboring cyclic acetal linkages, which was essentially complete in shortly ~60 min in ambient acidic media, quite shorter than ~540 min for the complete hydrolysis of PEMSD. However, the *ortho*-methoxy substitution of PEM*o*MSD slowed down this hydrolysis, which was essentially complete in ~180 min under the same conditions. Moreover, *Z*-isomerization remarkably slowed down this hydrolysis process. Under such conditions for 1800 min, the 62% *Z*-type PEM*o*MSD sample hydrolyzed 46%, similar to 37% hydrolysis of the 60% *Z*-type PEMSD sample, while the 61% *Z*-type PEM*p*MSD sample hydrolyzed up to 91%.

Moreover, the degree of hydrolysis of PEM*o*MSD samples varied from 100% to 33% in 570 min as changing the configuration from 100% *E*-type to 81% Z-type; the hydrolysis of the *E*-type units was accelerated but the hydrolysis of the *Z*-type units was slowed down on this light-triggered *Z*-isomerization.

This wide light tunability of acid sensitivity was induced by broadening the degree of light-triggered *Z*-isomerization and also electrodonating effects caused by a methoxy substituent in the different position of the aromatic rings of cinnamyl groups. This intriguing strategy provided a new molecular design of polymers for photosensors and light-tuned drug delivery applications.

The authors thank National Natural Science Foundation of China (20874081, 21074104), Research Fund for Doctoral Program of Higher Education of China (200805300004), Scientific Research Fund of Hunan Provincial Education Department (10A116), and Priority Academic Program Development of Jiangsu Higher Education Institutions for financial support of this work.

REFERENCES AND NOTES

1 Stuart, M. A. C.; Huck, W. T. S.; Genzer, J.; Müller, M.; Ober, C.; Stamm, M.; Sukhorukov, G. B.; Szleifer, I.; Tsukruk, V. V.; Urban, M.; Winnik, F.; Zauscher, S.; Luzinov, I.; Minko, S. *Nat. Mater.* **2010,** *9*, 101–113.

2 Roy, D.; Cambre, J. N.; Sumerlin, B. S. *Prog. Polym. Sci.* **2010,** *35*, 278–301.

3 Lee, M.; Jung, D.; Han, Y. *Mol. Cryst. Liq. Cryst.* **2006,** *444*, 41–50.

4 Iliopoulos, K.; Krupka, O.; Gindre, D.; Sallé, M. *J. Am. Chem. Soc.* **2010,** *132*, 14343–14345.

5 Moniruzzaman, M.; Sabey, C. J.; Fernando, G. F. *Polymer* **2007,** *48*, 255–263.

6 Yu, H.; Ikeda, T.; *Adv. Mater.* **2011,** *23*, 2149–2180.

7 Shimoboji, T.; Ding, Z.; Stayton, P. S.; Hoffman, A. S. *Bioconjug. Chem.* **2002,** *13*, 915–919.

8 Leclerc, E.; Furukawa, K. S.; Miyata, F.; Sakai, Y.; Ushida, T.; Fujii, T. *Biomaterials* **2004,** *25*, 4683–4690.

9 Nagasaki, T. *Drug Deliv. Syst.* **2008,** *23*, 637–643.

10 Wang, G.; Tong, X.; Zhao, Y. *Macromolecules* **2004,** *37*, 8911–8917.

11 Yagai, S.; Kitamuraa, A. *Chem. Soc. Rev.* **2008,** *37*, 1520–1529.

12 Zhao, Y. J. *Mater. Chem.* **2009,** *19*, 4887–4895.

13 Schumers, J.-M.; Fustin, C.-A.; Gohy, J.-F. *Macromol. Rapid Commun.* **2010,** *31*, 1588–1607.

14 Liu, J.; Chiu, Y. *J. Polym. Sci. Part A: Polym. Chem.* **2010,** *48*, 1142–1148.

15 Peris, S.; Tylkowski, B.; Ronda, J. C.; Garcia-Valls, R.; Reina, J. A.; Giamberini, M. *J. Polym. Sci. Part A: Polym. Chem.* **2009,** *47*, 5426–5436.

16 Qu, J.; Jiang, F.; Chen, H.; Sanda, F.; Masuda, T. *J. Polym. Sci. Part A: Polym. Chem.* **2009,** *47*, 4749–4761.

17 Lin, L.; Yan, Z.; Gu, J.; Zhang, Y.; Feng, Z.; Yu, Y. *Macromol. Rapid Commun.* **2009,** *30*, 1089–1093.

18 Wang, D.; Liu, J.; Ye, G.; Wang, X. *Polymer* **2009,** *50*, 418–427.

19 Barrio, J.; Oriol, L.; Alcalá, R.; Sánchez, C. *J. Polym. Sci. Part A: Polym. Chem.* **2010,** *48*, 1538–1550.

20 Yoshida, T.; Kanaoka, S.; Aoshima, S. *J. Polym. Sci. Part A: Polym. Chem.* **2005,** *43*, 5138–5146.

21 Jochum, F. D.; Borg, L.; Roth, P. J.; Theato, P. *Macromolecules* **2009,** *42*, 7854–7862.

22 Yu, B.; Jiang, X.; Wang, R.; Yin, J. *Macromolecules* **2010,** *43*, 10457–10465.

23 Lee, H.; Wu, W.; Oh, J. K.; Mueller, L.; Sherwood, G.; Peteanu, L.; Kowalewski, T.; Matyjaszewski, K. *Angew. Chem. Int. Ed.* **2007,** *46*, 2453–2457.

24 Kulawardana, E. U.; Kuruwita-Mudiyanselage, T.; Neckers, D. C. *J. Polym. Sci. Part A: Polym. Chem.* **2009,** *47*, 3318–3325.

25 Ventura, C.; Byrne, R.; Audouin, F.; Heise, A. *J. Polym. Sci. Part A: Polym. Chem.* **2011,** *49*, 3455–3463.

26 Jiang, J.; Tong, X.; Zhao, Y. *J. Am. Chem. Soc.* **2005,** *127*, 8290–8291.

27 Jiang, J.; Tong, X.; Morris, D.; Zhao, Y. *Macromolecules* **2006,** *39*, 4633–4640.

28 Babin, J.; Pelletier, M.; Lepage, M.; Allard, J.-F.; Morris, D.; Zhao, Y. *Angew. Chem. Int. Ed.* **2009,** *48*, 3329–3332.

29 Han, D.; Tong, X.; Zhao, Y. *Macromolecules* **2011,** *44*, 437–439.

30 Kang, M.; Moon, B. *Macromolecules* **2009,** *42*, 455–458.

31 Li, Y.; Jia, X.; Gao, M.; He, H.; Kuang, G.; Wei, Y. *J. Polym. Sci. Part A: Polym. Chem.* **2010,** *48*, 551–557.

32 Schumers, J.-M.; Gohy, J.-F.; Fustin, C.-A. *Polym. Chem.* **2010,** *1*, 161–163.

33 Muraoka, T.; Cui, H.; Stupp, S. I. *J. Am. Chem. Soc.* **2008,** *130*, 2946–2947.

34 Palmer, L. C.; Stupp, S. I. *Acc. Chem. Res.* **2008,** *41*, 1674–1684.

35 Jiang, X.; Lavender, C. A.; Woodcock, J. W.; Zhao, B. *Macromolecules* **2008,** *41*, 2632–2643.

36 He, J.; Tong, X.; Tremblay, L.; Zhao, Y. *Macromolecules* **2009,** *42*, 7267–7270.

37 Zhao, Y.; Tremblay, L.; Zhao, Y. *J. Polym. Sci. Part A: Polym. Chem.* **2010,** *48*, 4055–4066.

38 Palczewski, K.; Kumasaka, T.; Hori, T.; Behnke, C. A.; Motoshima, H.; Fox, B. A.; Trong, I. L.; Teller, D. C.; Okada, T.; Stenkamp, R. E.; Yamamoto, M.; Miyano, M. *Science* **2000,** *289*, 739–745.

39 Bohran, B.; Souto, M. L.; Imai, H.; Shichida, Y.; Nakanishi, K. *Science* **2000,** *288*, 2209–2212.

40 Dukkipati, A.; Kusnetzow, A.; Babu, K. R.; Ramos, L.; Singh, D.; Knox, B. E.; Birge, R. R. *Biochemistry* **2002,** *41*, 9842–9851.

41 Gascön, J. A.; Sproviero, E. M.; Batista, V. S. *Acc. Chem. Res.* **2006,** *39*, 184–193.

42 Li, Y.; Tang, Y.; Yang, K.; Chen, X.; Lu, L.; Cai, Y. *Macromolecules* **2008,** *41*, 4597–4606.

43 Kaihara, S.; Matsumura, S.; Fisher, J. P. *Macromolecules* **2007,** *40*, 7625–7632.

44 Zou, Y.; Brooks, D. E.; Kizhakkedathu, J. N. *Macromolecules* **2008,** *41*, 5393–5405.

45 Morinaga, H.; Morikawa, H.; Wang, Y.; Sudo, A.; Endo, T. *Macromolecules* **2009,** *42*, 2229–2235.

46 Chen, D.; Li, N.; Gu, H.; Xia, X.; Xu, Q.; Ge, J.; Lu, J.; Li, Y. *Chem. Commun.* **2010,** 6708–6710.

47 Gillies, E. R.; Fréchet, J. M. J. *Chem. Commun.* **2003,** 1640–1641.

48 Gillies, E. R.; Jonsson, T. B.; Fréchet, J. M. J. *J. Am. Chem. Soc.* **2004,** *126*, 11936–11943.

49 Gillies, E. R.; Fréchet, J. M. J. *Bioconjug. Chem.* **2005,** *16*, 361–368.

50 Griset, A. P.; Walpole, J.; Liu, R.; Gaffey, A.; Colson, Y. L.; Grinstaff, M. W. *J. Am. Chem. Soc.* **2009,** *131*, 2469–2471.

51 Chen, W.; Meng, F.; Li, F.; Ji, S.; Zhong, Z. *Biomacromolecules* **2009,** *10*, 1727–1735.

52 Ishigami, T.; Nakazato, K.; Uehara, M.; Endo, T. *Tetrahedron Lett.* **1979,** *20*, 863–866.

53 Lewis, F. D.; Elbert, J. E.; Upthagrove, A. L.; Hale, P. D. *J. Am. Chem. Soc.* **1988,** *110*, 5191–5192.

54 Cordes, T.; Schadendorf, T.; Lipp, M.; Rück-Braun, K.; Zinth, W. In Ultrafast Phenomena XVI, Springer Series in Chem. Phys.; Corkum, P.; Silvestri, S.; Nelson, K. A.; Riedle, E.; Schoenlein, R. W. Eds.; Springer-Verlag: Berlin; **2009,** *vol. 92*, pp 319–321.

55 Lewis, F. D.; Zuo, X. *J. Am. Chem. Soc.* **2003,** *125*, 2046–2047.

56 Lewis, F. D.; Zuo, X. *J. Am. Chem. Soc.* **2003,** *125*, 8806–8813.

57 Laschewsky, A.; Rekaï, E. D. *Macromol. Rapid Commun.* **2000,** *21*, 937–940.

58 Shi, Y.; Liu, G.; Gao, H.; Lu, L.; Cai, Y. *Macromolecules* **2009,** *42*, 3917–3926.

59 McLeary, J. B.; McKenzie, J. M.; Tonge, M. P.; Sanderson, R. D.; Klumperman, B. *Chem. Commun.* **2004,** 1950–1951.

60 McLeary, J. B.; Calitz, F. M.; McKenzie, J. M.; Tonge, M. P.; Sanderson, R. D.; Klumperman, B. *Macromolecules* **2004,** *37*, 2383–2394.

61 Yin, H.; Zheng, H.; Lu, L.; Liu, P.; Cai, Y. *J. Polym. Sci. Part A: Polym. Chem.* **2007,** *22*, 5091–5102.

62 Deng, J.; Shi, Y.; Jiang, W.; Peng, Y.; Lu, L.; Cai, Y. *Macromolecules* **2008,** *41*, 3007–3014.

63 Guo, A.; Liu, G.; Tao, J. *Macromolecules* **1996,** *29*, 2487–2493.

64 Ding, J.; Liu, G. *Chem. Mater.* **1998,** *10*, 537–542.

65 Sandholzer, M.; Bichler, S.; Stelzer, F.; Slugovc, C. *J. Polym. Sci. Part A: Polym. Chem.* **2008,** *46*, 2402–2413.

66 Yusa, S.-I.; Sugahara, M.; Endo, T.; Morishima, Y. *Langmuir* **2009,** *25*, 5258–5265.

67 Jiang, J.; Qi, B.; Lepage, M.; Zhao, Y. *Macromolecules* **2007,** *40*, 790–792.

68 Babin, J.; Lepage, M.; Zhao, Y. *Macromolecules* **2008,** *41*, 1246–1253.

69 Grovenstein, E., Jr.; Theophilou, S. P. *J. Am. Chem. Soc.* **1955,** *77*, 3795–3798.

70 Fife, T. H.; Jao, L. K. *J. Org. Chem.* **1965,** *30*, 1492–1495.

71 Benaglia, M.; Rizzardo, E.; Alberti, A.; Guerra, M. *Macromolecules* **2005,** *38*, 3129–3140.